Earthline Journal of Chemical Sciences
E-ISSN: 2581-9003; CODEN: EJCSB4
Volume 12, Number 3, 2025, Pages 331-342
https://doi.org/10.34198/ejcs.12325.331342

Effect of zirconium on Fox-7 – A DFT treatment

Lemi Türker

Department of Chemistry, Middle East Technical University, Üniversiteler, Eskişehir Yolu No: 1, 06800 Çankaya/Ankara, Turkey
e-mail: lturker@gmail.com; lturker@metu.edu.tr

Abstract

Interaction of 1,1-diamino-2,2-dinitroethylene (Fox-7) with zirconium atom has been investigated within the constraints of density functional theory mainly at the levels of B3LYP/ 6-31+G(d) and WB97X-D/ 6-31+G(d). Also, the interactions of zirconium with *cis*- and *trans*-amino nitro ethylenes (ANE, as substructures excerpted from Fox-7) are considered at the same levels of the theory. The results revealed that at the B3LYP/ 6-31+G(d) level *cis* and *trans*-amino nitro ethylenes decompose via different modes whereas Fox-7 structurally remains intact. Whereas WB97X-D/ 6-31+G(d) level of calculations yield decomposition via rupture of N-H bond in all the cases considered. The collected data revealed that all the optimized structures considered have exothermic heat of formation and favorable Gibbs free energy of formation values. They are thermally favored and electronically stable at the standard states. In all the cases the zirconium atom acquires positive partial charge and certain type of bonding happens with it and the organic partner. Various structural and quantum chemical data have been collected and discussed, including UV-VIS spectra.

1. Introduction

1,1-diamino-2,2-dinitroethylene (FOX-7) also known as DADE or DADNE [1-3] is an insensitive high explosive. Its explosive potential has been investigated thoroughly [4-18]. Compared to RDX, FOX-7 is much less sensitive in terms of impact, friction, and electrostatic discharge sensitivities [19]. Previous couple of decades has evidenced several FOX-7 based propellant formulations which have been developed in order to obtain propellant composites possessing reduced smoke production [20].

Certain metals are involved in various explosive formulations for instance, thermobaric weapons contain monopropellant or secondary explosive and additionally possess elements like B, Al, Si, Ti, Zr and C, mostly [21-28]. Titanium and zirconium, which are denser metal than magnesium and aluminum (a desirable factor for penetrators), were tested in various forms (gravel, washer, sponge). Also note that zirconium and its alloys are used to clad nuclear fuel rods due to their low neutron absorption. On the other hand, encapsulating aluminum with reactive metals such as magnesium, zirconium, and nickel or with polymers such as Teflon, Viton, and NC would also lower the ignition temperature and bridge the gap between microsecond detonation reactions and millisecond burning reactions [25,27].

The compositions of different energetic metallic particles and corresponding coatings are chosen in order to take advantage of the resulting exothermic reactions of alloying when the metals are combined or alloyed through heat activation. Bimetallic particles composed of a core/shell type structure of having different metals are to be properly chosen so that, upon achieving the melting point (for at least one of the metals) a relatively great deal amount of exothermic heat of alloying is liberated. The resulting bimetallic particles may be utilized

Received: July 3, 2025; Accepted: August 4, 2025; Published: August 7, 2025
Keywords and phrases: aminonitroethylenes, Fox-7, push-pull, zirconium, DFT.

as an enhanced blast additive by being dispersed within an explosive material [28]. The core metal can be one of aluminum, magnesium, boron, silicon, hafnium, or carbon. The outer shell metal/nonmetal is from nickel, zirconium, boron, titanium, sulfur, selenium, or vanadium.

Micron-sized zirconium (μZr) is a viable alternative fuel source for high-energy propellants. Liang *et al*, investigated the combustion performance of Zr-containing DAP-4-based composites. The results indicate that the introduction of μZr as a fuel in DAP-4 can improve the material's energy density and combustion characteristics [29].

2. Method of Calculations

In the present study, all the initial optimizations of the structures leading to energy minima have been achieved first by employing MM2 method which is then followed by semi empirical PM3 self consistent fields molecular orbital method [30-32]. Afterwards, the structure optimizations have been achieved within the framework of Hartree-Fock and finally by using density functional theory (DFT) at the levels of B3LYP/ 6-31+G(d) and WB97X-D/ 6-31+G(d) [33,34]. Note that the exchange term of B3LYP consists of hybrid Hartree-Fock and local spin density (LSD) exchange functions with Becke's gradient correlation to LSD exchange [35]. The correlation term of B3LYP consists of the Vosko, Wilk, Nusair (VWN3) local correlation functional [36] and Lee, Yang, Parr (LYP) correlation correction functional [37]. In the present study, the normal mode analysis for each structure yielded no imaginary frequencies for the 3*N*–6 vibrational degrees of freedom, where *N* is the number of atoms in the system. This search has indicated that the structure of each molecule considered corresponds to at least a local minimum on the potential energy surface. Furthermore, all the bond lengths have been thoroughly searched in order to find out whether any bond cleavage occurred or not during the geometry optimization process. All these computations were performed by using SPARTAN 06 program [38].

3. Results and Discussion

Aminonitroethylenes (ANE) could be in *cis*, *trans* or *geminal* isomeric forms. Figure 1 shows *cis* and *trans*-ANE which are two substructures obtainable from structure of Fox-7 (or from its zirconium composite).

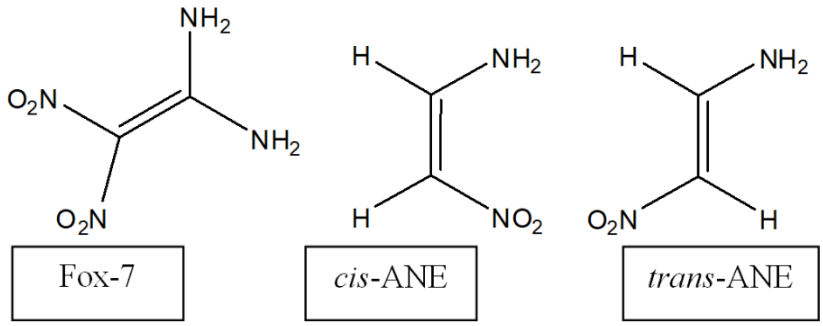

Figure 1. Structure of Fox-7 and two substructures obtainable from it.

Figure 2 shows optimized structures obtained from the zirconium composite of Fox-7. Note that the 1:1 zirconium composite of Fox-7, depending on the level of calculations, seemed either intact (B3LYP/ 6-31+G(d)) or decomposed (WB97X-D/ 6-31+G(d)). In the present treatment, the products from the parent composite are also named as composites and labeled accordingly as *cis* and *trans* zirconium composites (*cis*-ANE+Zr or *trans*-ANE+Zr). The optimizations based on two different functionals but the common basis set 6-31+G(d) which is a diffuse basis set [32]. Figures 2 and 3 stand for the various optimized structures obtained at

different levels of calculation, whereas the bond lengths/ distances of these structures can be found in Figures 4 and 5. According to the data obtained in the case of B3LYP/ 6-31+G(d), zirconium interacts with the NO_2 moiety of *cis*-ANE and the N-O bonds are highly disturbed (3.16 Å and 1.51 Å) whereas in the case of WB97X-D/ 6-31+G(d) level the zirconium atom prefers to attack the N-H bond of the amino group causing its cleavage (3.38 Å). On the other hand, WB97X-D/LANL2DZ level of calculation also reveals that the interaction of zirconium atom leads to cleavage of N-H bond (3.29 Å).

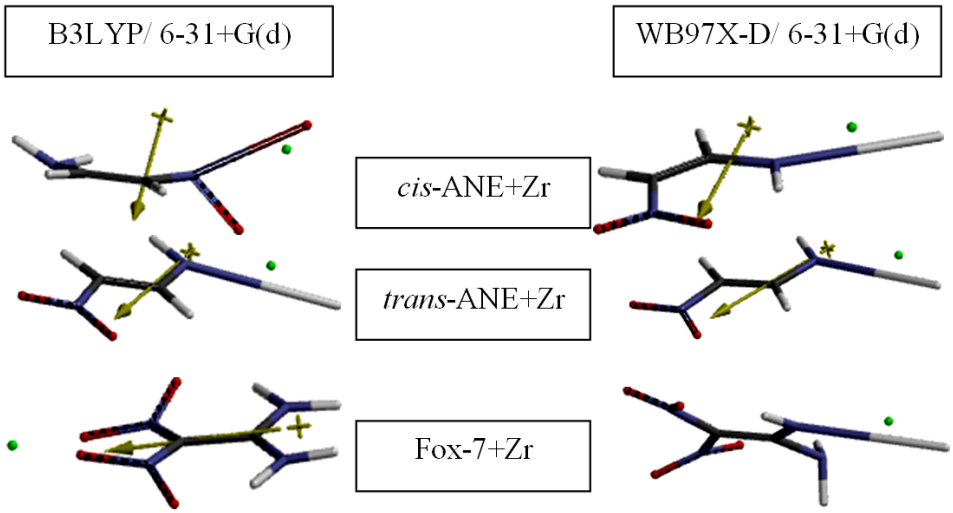

Figure 2. Optimized structures of the composites considered.

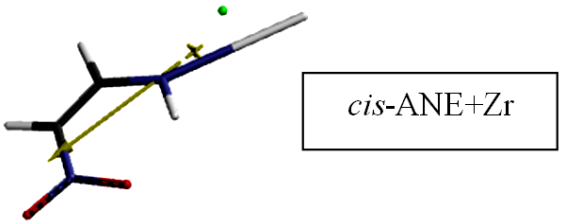

Figure 3. Optimized structure of *cis*-ANE+Zr composite considered (WB97X-D/ LANL2DZ).

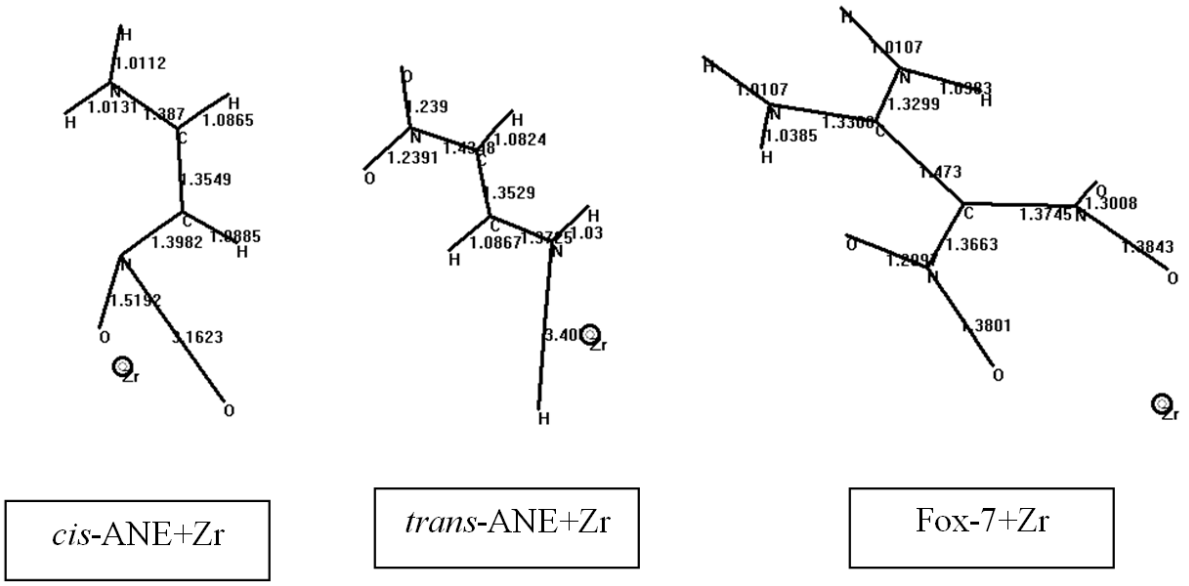

Figure 4. Calculated bond lengths/distances of composites considered (B3LYP/ 6-31+G(d)).

In the case of *trans*-ANE+Zr, the both levels of calculation indicate the rupture of N-H bond (see Figure 2). The N-H distance is 3.40 Å and 3.41 Å, respectively (see Figures 4 and 5).

As for the Fox-7+Zr composite, two opposing results have been obtained from the two different levels of calculation. Although, the composite seems to be intact in the case of B3LYP/ 6-31+G(d) level, the WB97X-D/ 6-31+G(d) type calculation shows the rupture of N-H bond (3.55 Å, see Figures 4 and 5). Also note that WB97X-D/ 6-31+G(d) level of calculations yield parallel results for the optimization processes, namely in each case N-H bond undergoes cleavage under the effect of zirconium atom.

Figure 3 shows the optimized structures of *cis*-ANE+Zr composite at the WB97X-D/ LANL2DZ) level of calculation. The structure exhibits quite a parallel appearance to result of WB97X-D/ 6-31+G(d) level of optimization. Whereas, the *trans* isomer resisted to converge during the optimization.

Figure 5 shows the calculated bond lengths/distances of composites considered (WB97X-D/ 6-31+G(d)).

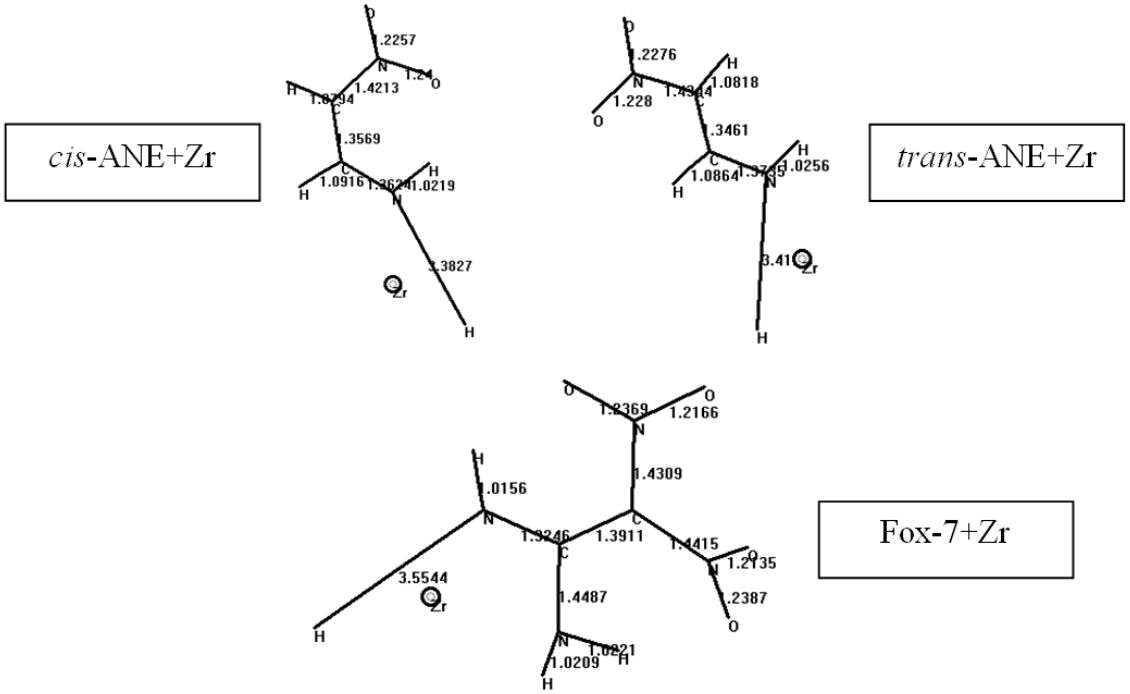

Figure 5. Calculated bond lengths/distances of composites considered (WB97X-D/ 6-31+G(d)).

Figure 6 shows the electrostatic potential (ESP) charges on the species presently considered. It is worth noting that the ESP charges are obtained by the program based on a numerical method that generates charges that reproduce the electrostatic potential field from the entire wavefunction [38].

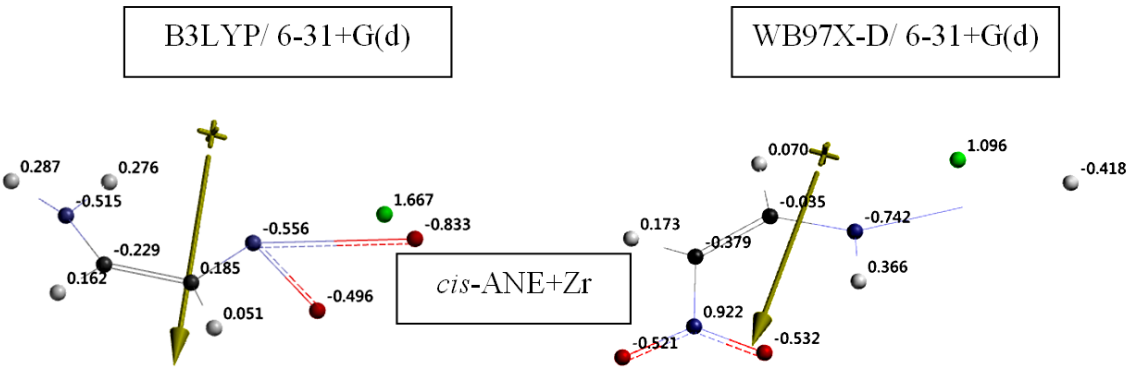

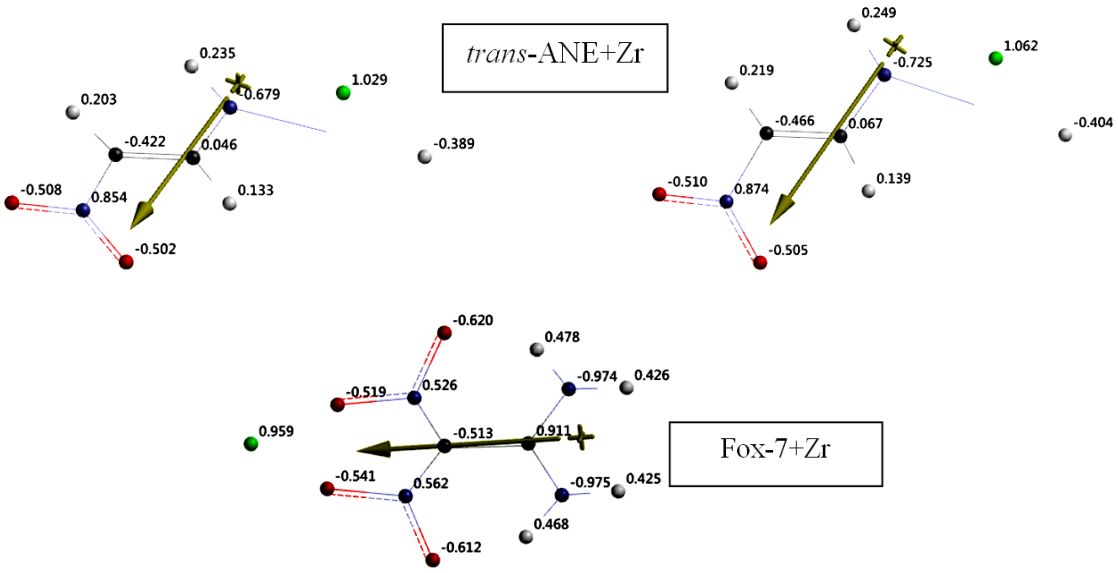

Figure 6. The ESP charges on the species presently considered.

The data shown in the figure reveal that with the exception of Fox-7+Zr composite in all the cases the zirconium atom possesses positive partial charge greater than unity which implies that the zirconium atom donates some electron population to the organic component acquiring itself some positive charge. Note that zirconium atom in the ground state possesses the electronic configuration of $[Ar]3d^{10}4s^24p^64d^25s^2$ [39]. In the case of *cis*-ANE+Zr, different levels of calculation yield completely different charge distributions. In the case of B3LYP/ 6-31+G(d) calculations, the rupture of N-O bond affects the pull-push character of the system. Compare the unexpected charges on carbon atoms, which are not in accord with the pull-push character of ANE. Whereas in WB97X-D/ 6-31+G(d) level of calculation pull-push character still remains.

Figure 7 shows the bond densities of the species presently considered (B3LYP/ 6-31+G(d)). As seen in the figure, in all the cases the zirconium atom is involved in certain type of bonding with the organic component. However, the participant atoms nearby the zirconium are different in each composite. The bond densities obtained at WB97X-D/ 6-31+G(d) level of calculations yielded similar patterns as the previous case (B3LYP/ 6-31+G(d)).

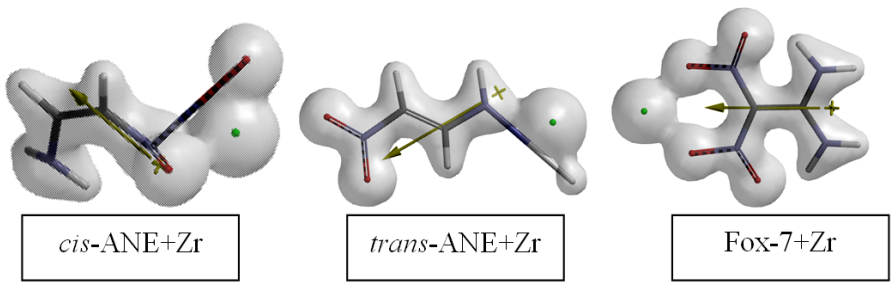

Figure 7. Bond densities of the species presently considered (B3LYP/ 6-31+G(d)).

Figure 8 shows the electrostatic potential maps of the species considered. The zirconium atom donates some electron population, it acquires partial positive charge and that positive field spreads over the whole system.

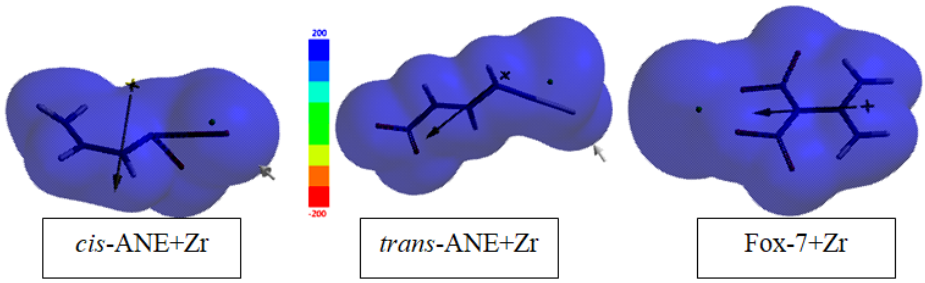

Figure 8. The electrostatic potential maps of the species considered (B3LYP/ 6-31+G(d)).

Figure 9 shows the local ionization potential maps of the species considered (B3LYP/ 6-31+G(d)). It is worth remembering that the local ionization potential map is a graph of the value of the local ionization potential on an isodensity surface corresponding to a van der Waals surface.

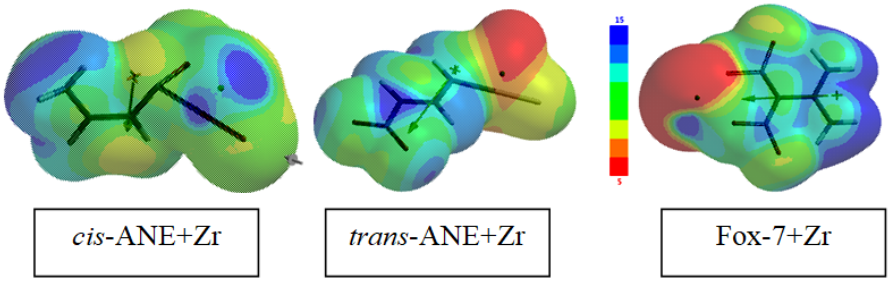

Figure 9. The local ionization potential maps of the species considered (B3LYP/ 6-31+G(d)).

Figure 10 displays the LUMO maps of the species presently considered (B3LYP/ 6-31+G(d)). Note that a LUMO map displays the absolute value of the LUMO on the electron density surface. The blue color (if any ists) stands for the maximum value of the LUMO and the red colored region, associates with the minimum value.

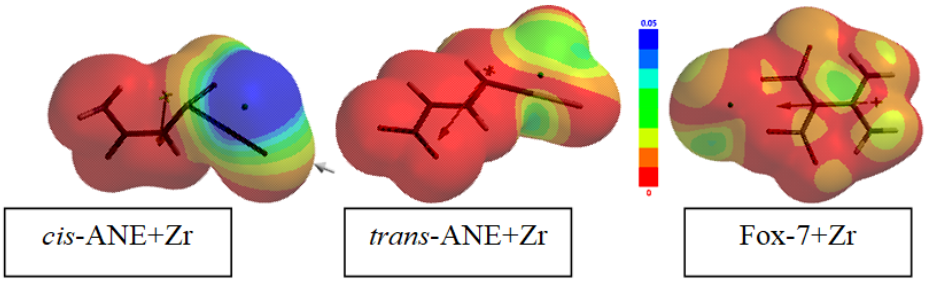

Figure 10. The LUMO maps of the species presently considered (B3LYP/ 6-31+G(d)).

Some thermo chemical properties of the species considered are presented in Tables 1 and 2. As seen in the tables, *cis*-ANE+Zr composite is more exothermic and more favorable than *trans*-ANE+Zr at the standard states.

Table 1. Some thermo chemical properties of the species considered (B3LYP/ 6-31+G(d) level).

Composite	H°	S° (J/mol°)	G°
cis-ANE+Zr	-1011005.07	361.59	-1011112.88
trans-ANE+Zr	-1010536.32	364.46	-1010644.99
FOX-7+Zr	-1692895.01	409.87	-1693017.21

Energies in kJ/mol.

Table 2. Some thermo chemical properties of the species considered (WB97X-D/ 6-31+G(d)).

Composite	Hº	Sº (J/molº)	Gº
cis-ANE+Zr	-1010198.751	357.55	-1010305.355
**cis*-ANE+Zr	-1009845.463	357.31	-1009951.996
trans-ANE+Zr	-1010190.436	361.64	-1010298.261

Energies in kJ/mol. FOX-7+Zr failed at this level for thermo chemical properties. *WB97X-D/ LANL2DZ) level of calculation.

Some energies of the species considered are shown in Tables 3 and 4. According to data in the tables, *cis*-ANE+Zr is more stable than *trans*-ANE+Zr at B3LYP/ 6-31+G(d) level but WB97X-D/ /6-31+G(d) level of calculations predict the reverse.

Table 3. Some energies of the species considered (B3LYP/ 6-31+G(d) level).

Composite	E	ZPE	E_C
cis-ANE+Zr	-1011200.59	183.29	-1011017.30
trans-ANE+Zr	-1010723.59	175.22	-1010548.37
Fox-7+Zr	-1693141.10	233.48	-1692907.62

Energies in kJ/mol.

Table 4. Some energies of the species considered (WB97X-D/ /6-31+G(d) level).

Composite	E	ZPE	E_C
cis-ANE+Zr	-1010389.47	179.73	-1010209.74
**cis*-ANE+Zr	-1010037.23	180.86	-1009856.37
trans-ANE+Zr	-1010381.08	178.86	-1010202.22

Energies in kJ/mol. * WB97X-D/ LANL2DZ)

Table 5 includes the HOMO, LUMO energies and interfrontier molecular orbital energy gap values (Δε) values of the species considered (B3LYP/ 6-31+G(d) level). Note that is $\Delta\varepsilon = \varepsilon_{LUMO}-\varepsilon_{HOMO}$. The data reveal that *trans*-ANE+Zr has lower HOMO and LUMO energy levels compared to the *cis* isomer. Consequently, the order of Δε values turn out to be *trans*-ANE+Zr < *cis*-ANE+Zr. Note that both of the isomers have been decomposed by the interaction with the zirconium atom, however the mode of interaction of Zr is different. In one case the nitro and in the other case the amino group undergoes bond cleavage. The electronic effects in the *cis* and *trans* isomers are under the influence of gross and fine topologies of the systems.

On the other hand, when the intact forms of *cis* and *trans* isomers are suitably constructed to form Fox-7 and let zirconium to interact with the system formed (multiple perturbation), due to the some extended conjugation effects the frontier molecular orbital energy levels of the resultant system become algebraically higher than the respective levels of the sub systems.

Table 5. The HOMO, LUMO energies and Δε values of the species considered (B3LYP/ 6-31+G(d) level).

Composite	HOMO	LUMO	Δε
cis-ANE+Zr	-490.85	-277.74	213.11
trans-ANE+Zr	-515.97	-348.56	167.41
Fox-7+Zr	-410.53	-242.48	168.05

Energies in kJ/mol.

Table 6 also shows the HOMO, LUMO energies and Δε values of some of the species considered but this time at the level of WB97X-D/ 6-31+G(d). The data reveal that in this case, the HOMO energy level of *trans*-ANE+Zr is lower than the corresponding level of *cis*-ANE+Zr. As for the LUMO energy levels the algebraic order is *cis*-ANE+Zr < *trans*-ANE+Zr. Then, the order of interfrontier molecular orbital energy gap (Δε) values become *cis*-ANE+Zr < *trans*-ANE+Zr. The opposing facts between the data presented in Tables 5 and 6 arise from the differences in internal configuration of the functionals employed in the calculations. Note that in both of the cases of calculations the basis set is common.

Table 6. The HOMO, LUMO energies and Δε values of some of the species considered (WB97X-D/ 6-31+G(d) level).

Composite	HOMO	LUMO	Δε
cis-ANE+Zr	-685.98	-148.78	537.20
trans-ANE+Zr	-696.79	-145.66	551.13

Energies in kJ/mol.

Figure 11 displays some of the molecular orbital energy levels of the composite species considered.

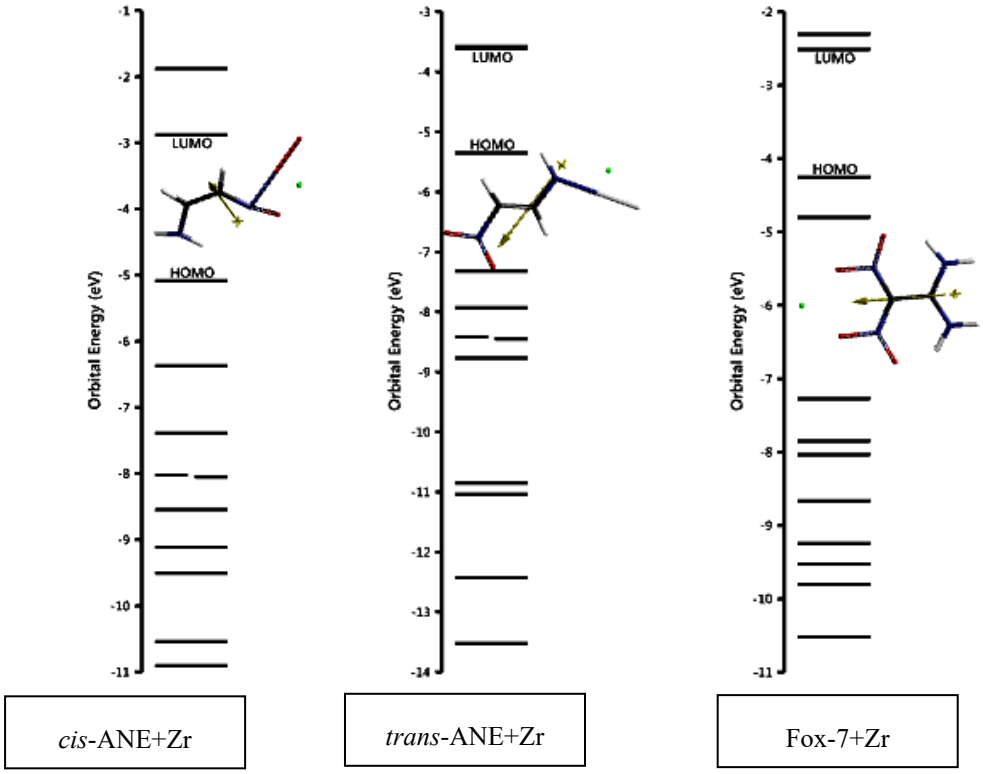

Figure 11. Some of the molecular orbital energy levels of the species considered (B3LYP/ 6-31+G(d) level).

Figure 12 shows the HOMO and LUMO patterns of the species presently considered (B3LYP/ 6-31+G(d)).

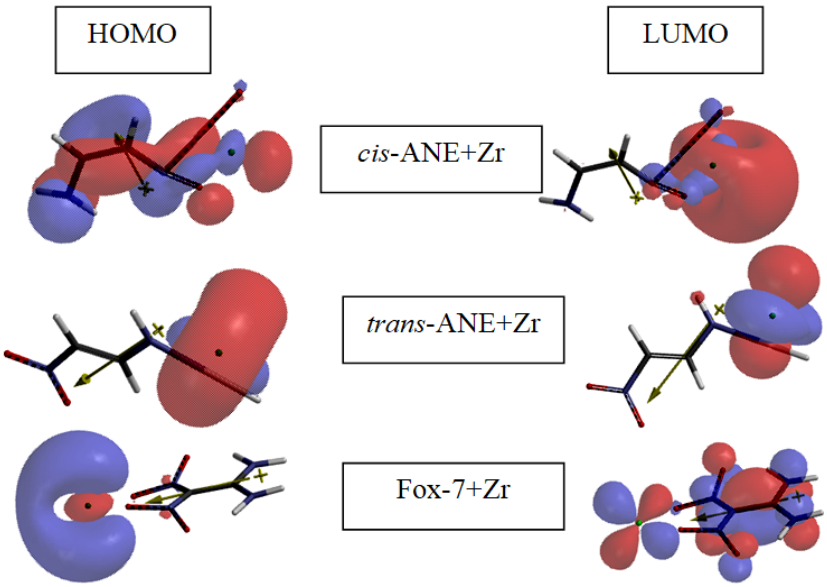

Figure 12. The HOMO and LUMO patterns of the species presently considered (B3LYP/ 6-31+G(d)).

Figure 13 stands for the HOMO and LUMO patterns of the isomeric species considered at WB97X-D/ 6-31+G(d) level. Note that the mode of decomposition of the isomeric species are different in Figures 12 and 13, thus a completely different patterns have been obtained for *cis*-ANE+Zr composite, whereas for *trans*-ANE+Zr isomer the HOMO and LUMO patterns are similar irrespective of the level of calculations.

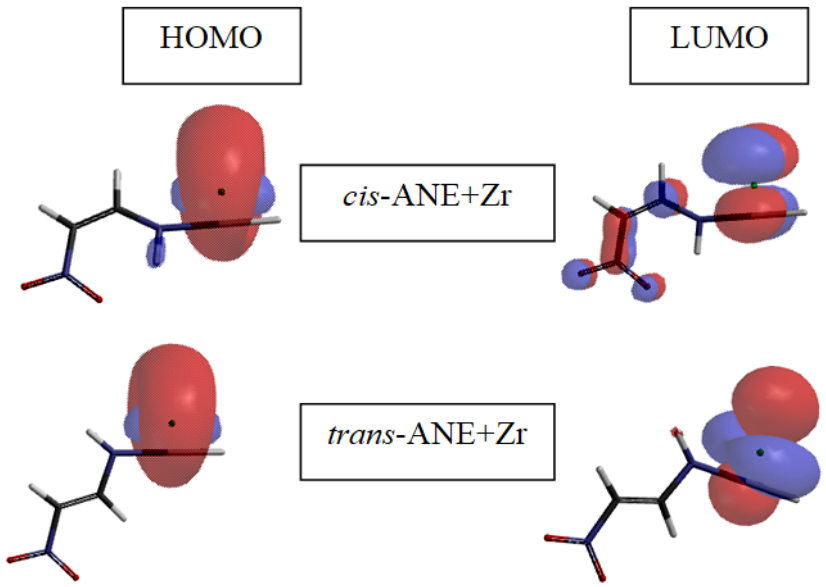

Figure 13. The HOMO and LUMO patterns of the isomeric species presently considered (WB97X-D/ 6-31+G(d)).

Figure 14 displays the calculated (time-dependent, TDDFT) UV-VIS spectrums of the species considered. As seen in the figure, spectrum of each specie exhibits calculation- level dependent appearance. Actually, the extended conjugation and kind of atoms involve in the extension dictates the emergence of the peaks and their positions and shape(s). The calculated intensities of the peaks are related to magnitudes of the transition moments varying from one (isomeric) structure to the other [40,41].

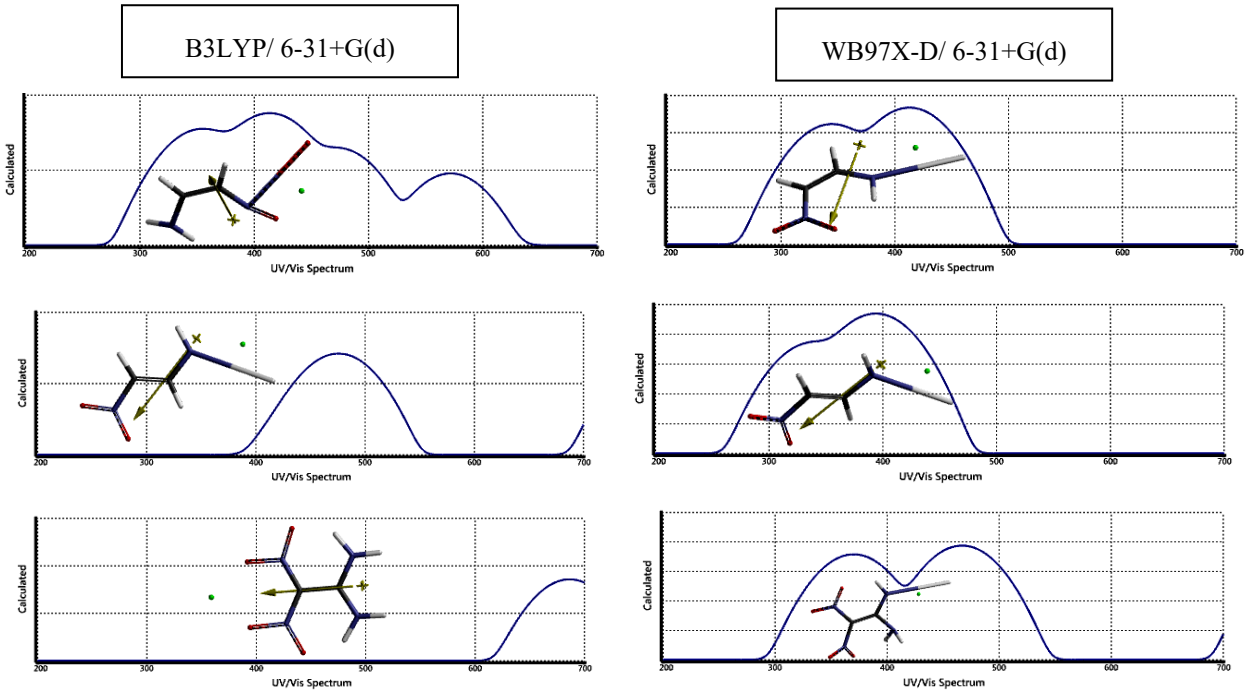

Figure 14. The calculated (TDDFT) UV-VIS spectrums of the species considered.

4. Conclusion

The computational study presently considered has focused on the interaction of zirconium atom with a well known explosive Fox-7 within the restrictions of DFT. Mainly two levels of theory, namely B3LYP/ 6-31+G(d) and WB97X-D/ 6-31+G(d) have been considered. The present results have indicated that the zirconium atom affects Fox-7 structure depending on the level of calculations (in the vacuum conditions). At B3LYP/ 6-31+G(d) level of calculations, although some substructures of Fox-7 decompose in the presence of the zirconium atom, the parent explosive (fox-7) remains almost intact. On the other hand, WB97X-D/ 6-31+G(d) calculations, in all the cases yield decomposed products which are consistent with each other in terms of the mode of decomposition that is the zirconium atom affects the N-H bond of Fox-7. All the structures decomposed or not are characterized with exothermic heat of formation and favorable Gibbs free energy of formation values and they are electronically stable. In every case the zirconium atom donates some electron population to the organic partner and forms a special type bonding, probably donor-acceptor type.

References

[1] Agrawal, J.P. (2010). *High energy materials* (1st ed.). Weinheim: Wiley-VCH. https://doi.org/10.1002/9783527628803

[2] Politzer, P., & Murray, J.S. (2003). *Energetic materials*, Part 1 (1st ed.). Amsterdam: Elsevier.

[3] Lochert, I.J. (2001). FOX-7 - A new insensitive explosive FOX-7. DSTO Aeronautical and Maritime Research Laboratory Australia, AR-012-065, November 2001.

[4] Latypov, N.V., Bergman, J., Langlet, A., Wellmar, U., & Bemm, U. (1998). Synthesis and reactions of 1,1-diamino-2,2-dinitroethylene. *Tetrahedron, 54*, 11525-11536. https://doi.org/10.1016/S0040-4020(98)00673-5

[5] Bemm, U., & Östmark, H. (1998). 1,1-Diamino-2,2-dinitroethylene: A novel energetic material with infinite layers in two dimensions. *Acta Crystallogr., C 54*, 1997-1999. https://doi.org/10.1107/S0108270198007987

[6] Latypov, N.V., Langlet, A., & Wellmar, U. (1999). New chemical compound suitable for use as an explosive, intermediate and method for preparing the compound. Patent No. WO99/03818.

[7] Östmark, H., Bergman, H., Bemm, U., Goede, P., Holmgren, E., Johansson, M., Langlet, A., Latypov, N.V., Petterson, A., Petterson, M.L., Wingborg, N., Vörde, C., Stenmark, H., Karlsson, L., & Hihkiö, M. (2001). 2,2-Dinitro-ethene-1,1-diamine (FOX-7) - Properties, analysis and scale-up. Paper presented at the 32nd International Annual Conference of ICT on Energetic Materials-Ignition, Combustion and Detonation, Karlsruhe, Germany.

[8] Östmark, H., Langlet, A., Bergman, H., Wingborg, N., Wellmar, U., & Bemm, U. (1998). FOX-7 – A new explosive with low sensitivity and high performance. Paper presented at The 11th International Detonation Symposium, Colorado, USA.

[9] Bergman, H., Ostmark, H., Pettersson, A., Petterson, M.L., Bemm, U., & Hihkio, M. (1999). Some initial properties and thermal stability of FOX-7. Paper presented at the Insensitive Munitions and Energetic Materials Symposium (NDIA), Tampa, Florida, USA.

[10] Trzciński, W.A., & Belaada, A. (2016). 1,1-Diamino-2,2-dinitroethene (DADNE, FOX- 7) – Properties and formulations (a Review). *Cent. Eur J. Energ. Mater*., *13*(2), 527-544.

[11] Janzon, B., Bergman, H., Eldsater, C., Lamnevik, C., & Ostmark, H. (2002). FOX-7 – A novel, high performance, low vulnerability high explosive for warhead applications. Paper presented at the 20th International Symposium on Ballistics, Orlando, Florida, USA, September 23-27.

[12] Matyushin, Y.N., Afanas'ev, G.T., Lebedev, V.P, Mahov, M.N., & Pepekin, V.I. (2003). TATB and FOX-7: Thermochemistry, performance, detonability, sensitivity. Paper presented at the 34th International Annual Conference of the Institute of Chemical Technology (ICT), Karlsruhe, Germany, June 24-27.

[13] Bellamy, A.J., Latypov, N.V., & Goede, P. (2004). Studies on the nitration of new potential precursors for FOX-7. Paper presented at the 7th Seminar on New Trends in Research on Energetic Materials, Pardubice, Czech Republic, April 20-22.

[14] Cudziło, S., Chyłek, Z., & Diduszko, R. (2005). Crystallization and characterization of 1,1-diamino-2,2-dinitroethene (DADNE). Paper presented at the 36th International Annual Conference of ICT, Karlsruhe, Germany, June 28-July 1.

[15] Trzciński, W.A., Cudziło, S., Chyłek, Z., & Szymańczyk, L. (2008). Detonation properties of 1,1-diamino-2,2-dinitroethene (DADNE). *Journal of Hazardous Materials, 157*(2-3), 605-612. https://doi.org/10.1016/j.jhazmat.2008.01.026

[16] Anniyappan, M., Talawar, M.B., Gore, G.M., Venugopalan, S., & Gandhe, B.R. (2006). Synthesis, characterization and thermolysis of 1,1-diamino-2,2-dinitroethylene (FOX-7) and its salts. *J. Hazard. Mater., B 137*, 812-819. https://doi.org/10.1016/j.jhazmat.2006.03.034

[17] Mishra, V.S., Vadali, S.R., Garg, R.K., Joshi, V.S., Wasnik, R.D., & Asthana, S. (2013). Studies on FOX-7 based melt cast high explosive formulations. *Cent. Eur J. Energ. Mater*., *10*(4), 569-580.

[18] Latypov, N.V., Johansson, M., Holmgren, E., Sizova, E.V., Sizov, V.V., & Bellamy, A.J. (2007). On the synthesis of 1,1-diamino-2,2-dinitroethene (FOX-7) by nitration of 4,6- dihydroxy-2-methylpyrimidine. *Org. Process Res. Dev*., *11*(1), 56-59. https://doi.org/10.1021/op068010t

[19] Klapötke, T.M. (2011). *Chemistry of high-energy materials* (1st ed.). Berlin: De Gruyter.

[20] Lips, H., & Menke, K. (2013). FOX-7/GAP rocket propellants for a shoulder launched projectile. Paper presented at the 27th International Symposium on Ballistics, Freiburg, Germany, April 22-26.

[21] Wildegger-Gaissmaier, A.E. (2003). Aspects of thermobaric weaponry. *ADF Health*, 2003, *4*, 3–6.

[22] Yen, N.H., & Wang, L.Y. (2012). Reactive metals in explosives. *Propellants Explosives Pyrotech., 37* (2), 143–155.

[23] Schaefer RA, Nicolich SM. (2005). Development and evaluation of new high blast explosives. In: 36th International Conference of ICT Karlsruhe, Germany, June 28–July 1, V9.

[24] Xing, X.L., Zhao, S.X., Wang, Z.Y., & Ge, G.T. (2014). Discussions on thermobaric explosives (TBXs). *Propellants Explos Pyrotech*., *39* (1), 14-17.

[25] Türker, L. (2016). Thermobaric and enhanced blast explosives (TBX and EBX). *Defence Technology*, *12*(6), 423-445. https://doi.org/10.1016/j.dt.2016.09.002

[26] Klapötke, T.M., Cudziło, S., Trzciński, W., A., & Paszula, J. (2024). Energy and blast performance of beryllium in a model thermobaric composition in comparison with aluminum and magnesium. *Defence Technology*, *36*, 13-19. https://doi.org/10.1016/j.dt.2024.02.011

[27] Jiao, X., Xu, Y., Zhou, T., Li, X., & Wu, Z. (2022). Enhancement of explosive effect of thermobaric explosive by metal reactive material. *Propellants, Explosives, Pyrotechnics, 48*(8), e202200351. https://doi.org/10.1002/prep.202200351

[28] Kellett, R.M. (2009). Exothermic alloying Al-Ni bimetallic nanoparticles dispersed within explosives. PCT Int. Appl., WO 2009046287 A1 20090409; 2009.

[29] Liang, K., Liu, Y., Hu, L., Liang, J., Lv, T., Wang, Y., & Hu, S. (2023). Effect of micron-sized zirconium powder on combustion decomposition behavior of molecular perovskite energetic material DAP-4. *Chemical Physics Letters*, 829, 140740. https://doi.org/10.1016/j.cplett.2023.140740

[30] Stewart, J.J.P. (1989). Optimization of parameters for semi-empirical methods I. *J. Comput. Chem.*, *10*, 209-220. https://doi.org/10.1002/jcc.540100208

[31] Stewart, J.J.P. (1989). Optimization of parameters for semi-empirical methods II. *J. Comput. Chem., 10*, 221-264. https://doi.org/10.1002/jcc.540100209

[32] Leach, A.R. (1997). *Molecular modeling*. Essex: Longman.

[33] Kohn, W., & Sham, L.J. (1965). Self-consistent equations including exchange and correlation effects. *Phys. Rev.*,*140*, 1133-1138. https://doi.org/10.1103/PhysRev.140.A1133

[34] Parr, R.G., & Yang, W. (1989). *Density functional theory of atoms and molecules*. London: Oxford University Press.

[35] Becke, A.D. (1988). Density-functional exchange-energy approximation with correct asymptotic behavior. *Phys. Rev. A*, *38*, 3098-3100. https://doi.org/10.1103/PhysRevA.38.3098

[36] Vosko, S.H., Wilk, L., & Nusair, M. (1980). Accurate spin-dependent electron liquid correlation energies for local spin density calculations: a critical analysis. *Can. J. Phys*., *58*, 1200-1211. https://doi.org/10.1139/p80-159

[37] Lee, C., Yang, W., & Parr, R.G. (1988). Development of the Colle-Salvetti correlation energy formula into a functional of the electron density. *Phys. Rev. B*, *37*, 785-789. https://doi.org/10.1103/PhysRevB.37.785

[38] SPARTAN 06 (2006). Wavefunction Inc. Irvine CA, USA.

[39] Glasstone, S., & Lewis, D. (1970). *Elements of physical chemistry*. London: Macmillan.

[40] Turro, N.J. (1991). *Modern molecular photochemistry.* Sausalito: University Science Books.

[41] Anslyn, E.V., & Dougherty, D.A. (2006). *Modern physical organic chemistry*. Sausalito, California: University Science Books.